

doi:10.3788/gzxb20164506.0616001

# $\beta$ -PTCDA 的电子结构和光学性质的第一性原理计算

王雪艳, 郑建邦, 李晓江, 曹崇德

(西北工业大学 理学院 陕西省光信息技术重点实验室, 西安 710072)

**摘要:** 基于密度泛函理论, 采用第一性原理赝势平面波方法研究了  $\beta$ -PTCDA 分子晶体的能带结构、分波态密度和光学性质, 通过分析不同种类原子的不同电子态在不同电子能级中的贡献, 获得  $\beta$ -PTCDA 分子晶体的光频介电常数、光吸收系数、折射率和能量损失函数等随光频的变化规律. 结果表明:  $\beta$ -PTCDA 作为一种直接带隙的窄带隙有机半导体, 对费米能级贡献较大的电子轨道为萘核的 C 2p 以及 O 2p 电子态, 即价带顶; 对导带底贡献较大的为 C 2p 及 O 2p 电子态, 包括酸酐 C 原子; 其在光子能量为 2~10 eV 的区域具有强的光吸收特性, 以及明显的双轴各向异性; 在介电函数实部  $\epsilon_1(\omega) < 0$  的光频区域,  $\beta$ -PTCDA 分子晶体具有各向异性电导率, 且与能量损失函数相一致.

**关键词:** 能带结构; 态密度; 光学性质; 密度泛函理论;  $\beta$ -PTCDA 分子晶体

**中图分类号:** O48; O43; O469

**文献标识码:** A

**文章编号:** 1004-4213(2016)06-0616001-8

## Electronic Structures and Optical Properties of $\beta$ -PTCDA Based on the First-Principles Investigation

WANG Xue-yan, ZHENG Jian-bang, LI Xiao-jiang, CAO Chong-de

(Shaanxi Key Laboratory of Optical Information Technology, Department of Applied Physics, School of Science, Northwestern Polytechnical University, Xi'an 710072, China)

**Abstract:** Electronic band structure, Partial Density of States (PDOS) and optical properties of  $\beta$ -phase 3, 4, 9, 10-perylenetetracarboxylic dianhydride ( $\beta$ -PTCDA) molecular crystal were systematically investigated by first-principles calculations based on Density Functional Theory (DFT). The contribution of different type of atoms electronic states to different electronic levels was analyzed, and the frequency dependent optical functions such as the dielectric function, absorption coefficient, refractive index and energy loss function of  $\beta$ -PTCDA molecular crystal that changed with optical frequency were analyzed and obtained. The results showed that  $\beta$ -PTCDA is a direct narrow band gap semiconductor, and the electron orbit making larger contribution to the Fermi level is the O 2p electronic state and C 2p electronic state that come from the perylene core, which are also the top of valence band; what makes larger contribution to the bottom of the conduction band is also the C 2p and O 2p electronic states, including anhydride C atoms; in the photon energy range of 2 to 10 eV, the strong light absorption and obvious biaxial anisotropy can be observed. In the optical frequency range with the real part of dielectric function  $\epsilon_1(\omega) < 0$ ,  $\beta$ -PTCDA molecular crystal has an anisotropic conductivity, which is consistent with the energy loss function.

**Key words:** Band structure; PDOS; Optical properties; DFT;  $\beta$ -PTCDA molecular crystal

**OCIS Codes:** 000.3860; 230.0250; 160.4760; 300.6470; 300.1030

**Foundation item:** The Doctorate Foundation of Northwestern Polytechnical University (No. CX201324), the National Natural Science Foundation of China (Nos. 51471135, 51171152) and the Seed Foundation of Innovation and Creation for Graduate Students in Northwestern Polytechnical University (No. Z2015144).

**First author:** WANG Xue-yan (1983—), female, Ph. D. degree candidate, mainly focuses on optoelectronic information materials & technology. Email: xueyanadeline@163.com

**Responsible author (Corresponding author):** ZHENG Jian-bang (1965—), male, professor, Ph. D. degree, mainly focuses on nonlinear optics and low dimensional optoelectronic devices and technology. Email: zhengjianbang@nwpu.edu.cn

**Received:** Jan. 11, 2016; **Accepted:** Mar. 24, 2016

<http://www.photon.ac.cn>

## 0 Introduction

Within the field of organic semiconductor material,  $\beta$ -phase 3, 4, 9, 10-perylenetetracarboxylic dianhydride ( $\beta$ -PTCDA) derived from perylene is an important optical material and has attracted much interest due to its large technological potential<sup>[1-2]</sup>.  $\beta$ -PTCDA, as a photochemically stable dye pigment, is usually used as an organic light-emitting dopant, fluorescent dye, organic photovoltaic and organic field effect transistor material<sup>[3-4]</sup>. It is also used as a  $n$ -type semiconductor due to the highly charge carrier mobility<sup>[5-6]</sup>.  $\beta$ -PTCDA is one of the materials with the brightest development prospects that can dominate future organic electronics and optoelectronic devices<sup>[4, 7-8]</sup>.  $\beta$ -PTCDA, as an oligomer, easily forms well-ordered crystalline structure and could serve as model systems, and thus the properties of organic semiconductor could be well understood, especially the mechanisms governing charge transport and electron spin polarization transport. PTCDA molecule, as one of the typical planar molecules with extended  $\pi$ -systems, has the possibility of controllable self-assembly of ordered thin films that lead to a strong improvement in device performances<sup>[9]</sup>.

The good  $\beta$ -PTCDA molecular crystal thin film was prepared in our experimental group. The physical properties of  $\beta$ -PTCDA film are directly or indirectly correlated to the electronic structures, such as the band structure and Density of States (DOS), of  $\beta$ -PTCDA molecular crystal<sup>[10]</sup>. For example, the polarized absorption, energies of electronic transitions and other semiconducting properties are closely related with it. Much work have been reported in the aspect of electronic structures of several monolayer PTCDA films rather than PTCDA molecular crystal<sup>[11-12]</sup>. S. Sharifzadeh *et al.* has briefly reported the optical spectra of bulk PTCDA, but the report did not explore the relationships between the electronic structure and optical properties, such that the electronic structures and optical properties of PTCDA molecular crystal were still not thoroughly understood<sup>[13-14]</sup>, especially the causal relationship between them. To understand the relationship on the electronic structures and optical properties in detail knowledge about the PTCDA molecular crystal was indispensable.

In the bulk, PTCDA crystallizes in stacked molecular sheets, each plane of which contains interlocking molecules in a herringbone structure that is stabilized by dispersion forces and the electrostatic interactions between their quadrupole moments. Two monoclinic polymorphs have been observed, which were referred to as a  $\alpha$ - and  $\beta$ -phase<sup>[15-16]</sup>. In this paper,

calculations on the electronic structures and optical properties of  $\beta$ -PTCDA molecular crystal were carried out by the first-principles based on Density Functional Theory (DFT). The  $\beta$ -PTCDA molecular crystal was geometrically optimized, after which its electronic band structure, PDOS and anisotropic optical properties were presented and analyzed systematically; particularly, more emphases were put on the intrinsic relationship between its electronic structures and optical properties, from which its semiconductor properties and optical anisotropy were comprehended completely.

## 1 Computational details

The structure model of  $\beta$ -PTCDA molecular crystal was taken from the literature<sup>[15]</sup>. After carefully geometry optimization, a good structure of  $\beta$ -PTCDA molecular crystal was obtained ( $a$ : 0.371 nm,  $b$ : 1.944 nm,  $c$ : 1.225 nm,  $\alpha = \gamma = 90^\circ$ ,  $\beta = 59.9^\circ$ ). This model had  $P2_1/c$  symmetry monoclinic system and with two molecules in each unit cell<sup>[17]</sup>. The electronic structures and optical properties of  $\beta$ -PTCDA molecular crystal were systematically studied by DFT calculations using the CASTEP (Cambridge Sequential Total Energy Package) module of Materials Studio package<sup>[18]</sup>. The soft compressibility was adopted for this crystal in the geometry optimization process. All calculations were performed using the Perdew-Burke-Ernzerhof (PBE) functional, which described the electronic exchange and correlation within a Generalized Gradient Approximation (GGA)<sup>[19-20]</sup>. In addition, the latest norm conserving pseudopotential generation technology in reciprocal space was adopted for plane wave basis set with a cutoff energy of 880 eV, using a Self-Consistent-Field (SCF) convergence threshold of  $5.0 \times 10^{-7}$  eV/atom, which could guarantee the accuracy

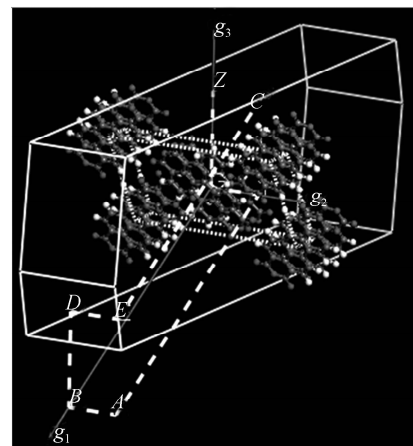


Fig. 1 The  $\beta$ -PTCDA molecular crystal in reciprocal space, with the gray, red and white balls representing C, O and H atoms, respectively. The dash line Z-G-Y-A-B-D-E-C gives the first Brillouin zone.

of the Kramers-Kronig transformation. This condition ensured that the scattering properties of the pseudopotential were reproduced correctly and had been tested to be accurate and reliable for  $\beta$ -PTCDA molecular crystal. All the integrations in the first Brillouin zone (Fig. 1) were performed on the path determined by the monoclinic scheme and the Monkhorst-Pack grid with  $k$ -point separation of  $0.007 \text{ nm}^{-1}$ [21]. The electronic configurations were treated as C  $2s^2 2p^2$ , O  $2s^2 2p^4$  and H  $1s^1$ .

The DFT calculated band gap of  $\beta$ -PTCDA molecular crystal was slightly smaller than that in experimental measurements, so the calculated optical properties would be wrongly estimated. In order to overcome the deficiency, the scissors operator was used in plotting the electronic band structure and PDOS and calculating the dielectric functions. The method used for the calculation of electronic structures and optical properties has been proven to be reasonable and consistent with corresponding experimental results in a series of previous literatures[22-23] and in our absorption spectrum. This would provide the useful information concerning the electronic structures and optical properties of  $\beta$ -PTCDA molecular crystal.

## 2 Results and discussion

### 2.1 Band structure and density of states

The electronic band structure of  $\beta$ -PTCDA molecular crystal was plotted along the path in the Brillouin zone and shown in Fig. 2, where the Fermi level ( $E_F$ ) was set to zero. The band structure provided a useful tool for qualitative analysis of the electronic structure of  $\beta$ -PTCDA molecular crystal, which was of great importance in understanding the properties of  $\beta$ -PTCDA organic semiconductor. For example, the band structure showed an obvious band gap that characterized the semiconductor[13, 24]; the relatively flat and dispersionless bands near the Fermi level was likely contributed to optical absorption strongly as a result of electronic interband transitions; the upper conduction bands and lower valence bands fluctuated obviously, which was attributed to the strong electronic hybridizations. As an organic molecular crystalline semiconductor, the  $\beta$ -PTCDA energy gap was estimated as 2.116 eV by scissoring 0.85 eV operators, which was just comparable with its optical band gap and basically reflected its fundamental transitions[14, 25]. From the enlarged details of the band structure we can clearly see that the bottom of the

conduction band and the top of valence band are located at the same point of  $k$ -space, it can be judged that  $\beta$ -PTCDA molecular crystal is a direct bandgap semiconductor.

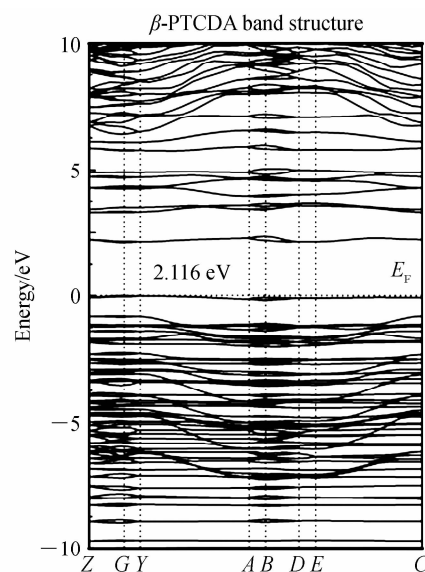
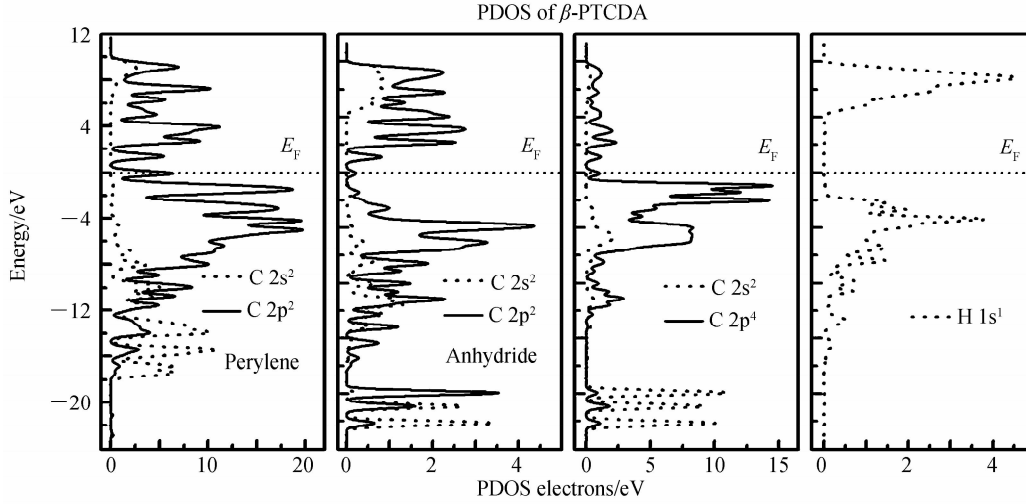


Fig. 2 The electronic band structures of  $\beta$ -PTCDA

The PDOS pictures (Fig. 3) allow a distinguishingly different atomic orbital of electronic hybridization, clearing the nature of the interaction and detailing the different electronic states distribution through the electron energy level in  $\beta$ -PTCDA molecular crystal. In order to clearly analyze the electron structures of  $\beta$ -PTCDA molecular crystal and comprehend other physical properties of it in combination with the PDOS of  $\beta$ -PTCDA molecular crystal, it can be seen that a band at  $E_F$  mainly originated from C  $2p$  electronic states in perylene core and O  $2p$  electronic states, as the top of valence band; the upper valence bands from  $-7$  to  $-0.8$  eV were mainly derived from C  $2p$  (containing perylene core and anhydride C atoms), O  $2p$  and H  $1s$  electron orbital hybridization that was shaped like parabola; the lower valence bands did not affect its physical properties so that the remote electronic distributions could be ignored; the band at the lowest conduction band was also derived from C  $2p$  and O  $2p$  electronic states; the higher conduction bands located at about 3 to 6 eV were predominantly composed of C  $2p$  and O  $2p$  electronic states that were slightly hybridized; and the bands from 6 to 10 eV were derived from the non-localized C  $2s2p$  (both perylene core and anhydride C atoms), O  $2p$  and H  $1s$  electron orbital, which showed strong hybridizations that were shaped like saddles, known as sp-like bands.


 Fig. 3 Partial density of states of  $\beta$ -PTCDA molecular crystal

## 2.2 Optical properties

The optical properties of  $\beta$ -PTCDA molecular crystal that were due to electronic interband transitions were calculated and analyzed intensively, including the dielectric function, reflectivity, absorption coefficient, refractive index and optical conductivity.

The dielectric function ( $\epsilon(\omega) = \epsilon_1(\omega) + i\epsilon_2(\omega)$ ) was an important function to describe the optical properties, from which others optical parameters could be derived. The dielectric response largely relied on the electronic structure of material, such as band structures and electronic density of states. By the electronic-dipole approximation, the imaginary part  $\epsilon_2(\omega)$  as the pandect of optical properties was calculated from the momentum matrix elements between the occupied and unoccupied wave functions within selection rules<sup>[26]</sup>, as shown in Eq. (1)<sup>[27-28]</sup>

$$\epsilon_2(\omega) = \frac{2e^2\pi}{\Omega\epsilon_0} \sum_{k,v,c} |\langle \Psi_k^c | \mathbf{u} \cdot \mathbf{r} | \Psi_k^v \rangle|^2 \cdot \delta(E_k^c - E_k^v - \hbar\omega) \quad (1)$$

where,  $\mathbf{u}$  was the electric-field vector of the polarization of the incident light field, and  $\mathbf{r}$  was the position operator and expressed as momentum matrix to satisfy the crystalline boundary condition used in the calculations<sup>[29]</sup>. The superscripts  $c$  and  $v$  represented the conduction and valence bands, respectively,  $\omega$  was the frequency of incident photons,  $\Omega$  was the volume of crystal cell, and  $\epsilon_2(\omega)$  reflected the electrons transitions between occupied and unoccupied bands obeying the selection rules<sup>[30]</sup>. The real part  $\epsilon_1(\omega)$  was calculated by the Kramers-Kronig transformation, as shown in Eq. (2)

$$\epsilon_1(\omega) = 1 + \frac{2}{\pi} P \int_0^\infty \frac{\omega' \epsilon_2(\omega')}{\omega'^2 - \omega^2} d\omega' \quad (2)$$

where,  $P$  denoted the principle value of the integral. Other optical constants can be derived from the dielectric function, for example, the absorption

coefficient  $\alpha(\omega)$  was given by Eq. (3); reflectivity  $R(\omega)$  was given by Eq. (4); the optical conductivity  $\delta(\omega)$  was obtained according to the Eq. (5); the refractive index could be derived from Eq. (6)<sup>[31-32]</sup>; The loss function could be derived from Eq. (7)<sup>[33]</sup>

$$\alpha(\omega) = \sqrt{2} \omega [\sqrt{\epsilon_1^2(\omega) + \epsilon_2^2(\omega)} - \epsilon_1(\omega)]^{1/2} \quad (3)$$

$$R(\omega) = \left| \frac{\sqrt{\epsilon_1(\omega) + j\epsilon_2(\omega)} - 1}{\sqrt{\epsilon_1(\omega) + j\epsilon_2(\omega)} + 1} \right|^2 \quad (4)$$

$$\delta(\omega) = \delta_1(\omega) + i\delta_2(\omega) = -i \frac{\omega}{4\pi} [\epsilon_1(\omega) + i\epsilon_2(\omega) - 1] \quad (5)$$

$$N(\omega) = n(\omega) + ik(\omega) = [\sqrt{\epsilon_1^2(\omega) + \epsilon_2^2(\omega)} + \epsilon_1(\omega)]^{1/2} / \sqrt{2} + i[\sqrt{\epsilon_1^2(\omega) + \epsilon_2^2(\omega)} - \epsilon_1(\omega)]^{1/2} / \sqrt{2} \quad (6)$$

$$L(\omega) = \text{Im} \left( \frac{-1}{\epsilon(\omega)} \right) = \frac{\epsilon_2(\omega)}{\epsilon_1^2(\omega) + \epsilon_2^2(\omega)} \quad (7)$$

In the calculations, the optical properties were analyzed under the polarized light mode. For the polarization directions of  $E // g_2$  and  $E // g_3$ , the calculated optical properties were similar, but were obviously different from those of  $E // g_1$ , which clearly indicated the anisotropic behaviors of  $\beta$ -PTCDA molecular crystal<sup>[13]</sup>. The frequency-dependent dielectric functions projected along three principal directions, as shown in Fig. 4. The calculated static dielectric constants  $\epsilon_1(0)$  were 2.79, 5.68 and 6.20 for  $\beta$ -PTCDA along  $g_1$ ,  $g_2$  and  $g_3$  directions, respectively, which characterized the dielectric response of  $\beta$ -PTCDA in the static electric field. The imaginary part  $\epsilon_2(\omega)$  of dielectric function for the  $\beta$ -PTCDA basically reflected the electronic transitions from valence bands to the conduction bands that satisfied the selection rules within the sub-bands, which reflected the solid band structure and were responsible for intrinsic absorption, as shown in Fig. 5(a). Although the reflectivity spectra took place in the same energy range as the absorption

coefficients, as shown in Fig. 5(b), the reflectivity was relatively weak, and particularly in the photon energy

range of 2~10 eV, obvious biaxial anisotropy can be observed.

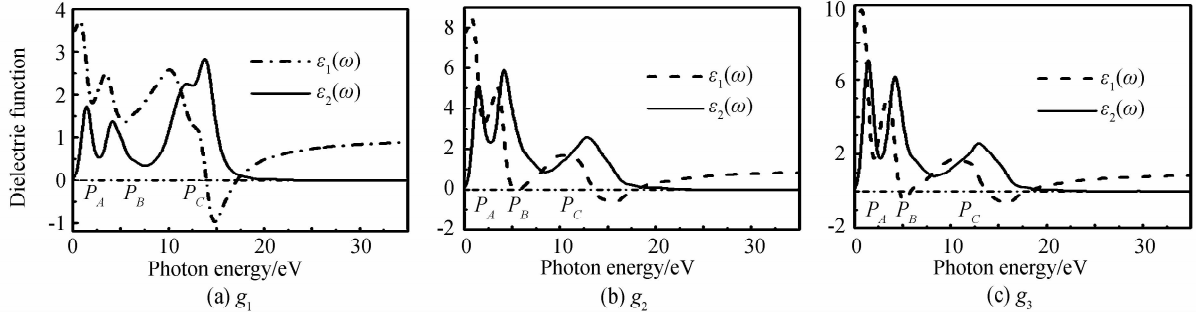


Fig. 4 Dielectric Function of  $\beta$ -PTCDA molecular crystal

In the optical frequency region, when the real part  $\epsilon_1(\omega)$  of dielectric function was at a valley value, the imaginary part  $\epsilon_2(\omega)$  would be at a peak value, which corresponded to the electron transition resonance absorption. In a certain optical frequency range, the real part  $\epsilon_1(\omega) < 0$ , showed that its conductivity was bigger, and also was a reflection of the surface plasmon polariton. As for the dielectric function  $\epsilon_1(\omega)$  shown in Fig. 4, the photo energy ranges of  $\epsilon_1(\omega) < 0$  in  $g_2$  and  $g_3$  polarization directions were [13.6 eV, 18 eV], which were different from that in  $g_1$  direction [14 eV, 17 eV]. This suggests that the  $\beta$ -PTCDA molecular crystal had anisotropic conductivity, which was perfectly consistent with the energy loss function. Three clear peaks ( $P_A$ ,  $P_B$  and  $P_C$ ) of  $\epsilon_2(\omega)$  in the range of 2~18 eV were respectively attributed to the electronic transition between O 2p states in the highest valence band and C 2p states in the lowest conduction band as labeled peak A ( $P_A$ ); C and O sp hybridization states in the sub-high valence band located above 5 eV and C 2p states in the lowest conduction band as labeled peak B ( $P_B$ ); C 2s2p and O 2p states in the middle valence bands located at about 10 eV and C 2p states in the middle conduction band as labeled peak C ( $P_C$ ). It can be seen that  $P_C$  in  $g_1$  direction was in split doublet form, which was contributed by two electrons of O 2p states, and there was only one electron from O 2p states in  $g_2$  and  $g_3$  directions due to the crystal field effect, respectively.

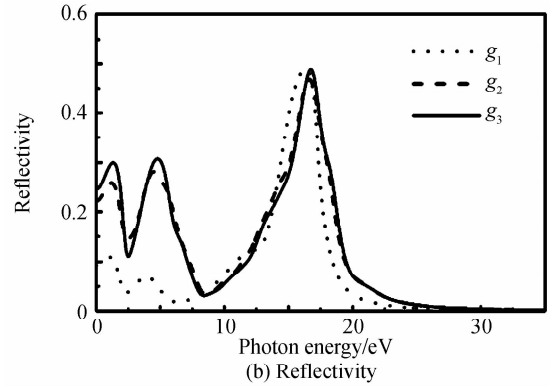
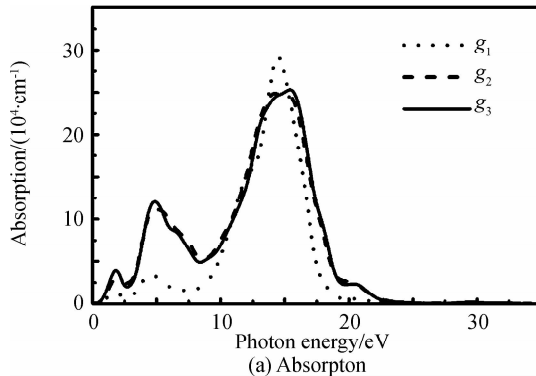


Fig. 5 Absorption and reflectivity of  $\beta$ -PTCDA molecular crystal

The visible light absorption spectrum of  $\beta$ -PTCDA film from the experimental study gave an absorption range of 600~400 nm (2.01~3.01 eV). The absorption edge at 2.01 eV was in accordance with the band gap of it<sup>[34]</sup>. These excitations may be attributed to the shifting of electrons from C 2p and O 2p states in higher valence bands to C 2p states in lower conduction bands. Moreover, based on the results of calculations (Fig. 5 (a)), the optical absorption peak in the low-energy region at about 2.5 eV corresponded to the visible optical absorption spectrum. The peak at about 5.5 eV corresponded to the ultraviolet absorption, and the peak at about 15.8 eV corresponded to a part of low frequency super ultraviolet or extreme ultraviolet absorption. Besides, a significant phenomenon of optical anisotropy was observed in the ultraviolet-visible light region of 2 to 10 eV. Nevertheless, no noteworthy absorption and reflectivity occurred at photon energy beyond 25 eV, namely, when the photon energy was higher than 25 eV, the  $\beta$ -PTCDA molecular crystal would become transparent. The photons had full conductivities with no absorption and reflectivity, which showed that the imaginary part of conductivity tended to 1 (Fig. 6), and the real part  $n$  of refractive index tended to 1, the imaginary part  $k$  to 0 (Fig. 7).

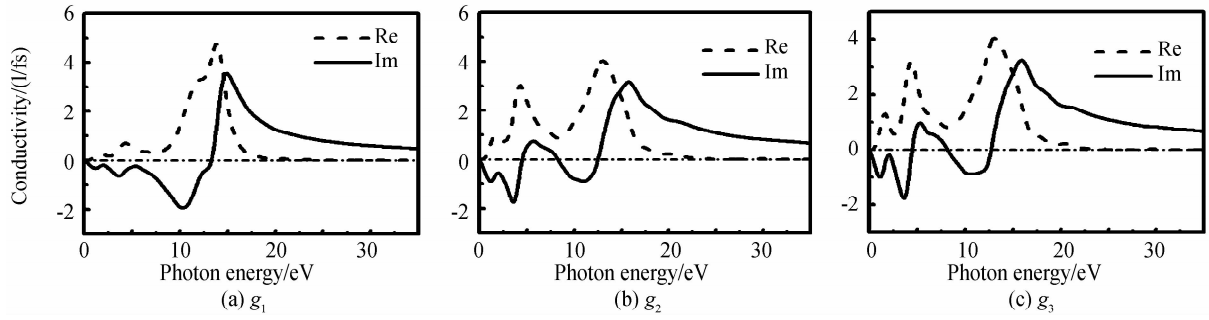


Fig. 6 Conductivity of  $\beta$ -PTCDA molecular crystal

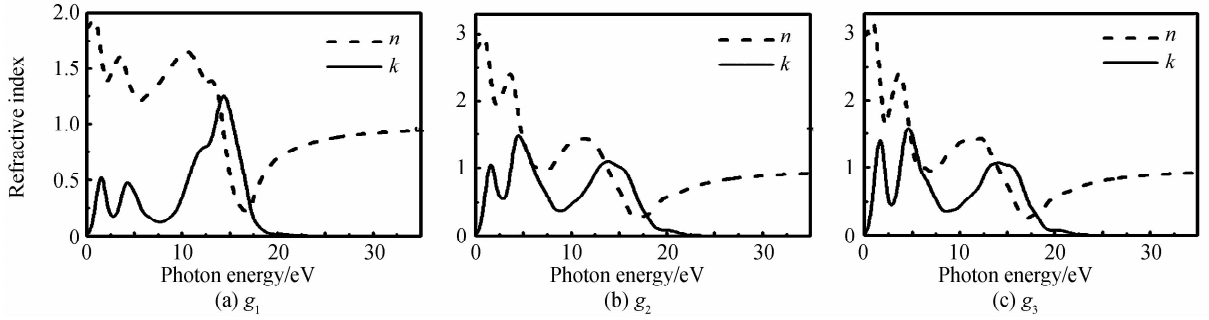


Fig. 7 Refractive Index of  $\beta$ -PTCDA molecular crystal

Furthermore, the optical properties depended rather strongly on the crystallographic orientation of  $\beta$ -PTCDA. This suggested that one could use these distinct optical features to characterize the crystallographic orientation the  $\beta$ -PTCDA film<sup>[35]</sup>. It can be seen from Fig. 5 that the absorption and reflectivity along the polarization direction of  $E // g_1$  were lower than those of  $E // g_2$  and  $E // g_3$  in a photon energy range of 0~10 eV, which indicated that the photon absorption and reflectivity were mainly attributed to  $E // g_2$  and  $E // g_3$  in the ultraviolet-visible light region<sup>[23]</sup>. These were just the embodiments of optical anisotropy of  $\beta$ -PTCDA molecular crystal.

The anisotropy of the refractive index was shown in Fig. 7, from which we derived that the static refractive indexes  $n(0)$  were 1.67, 2.38 and 2.49 for  $\beta$ -PTCDA along  $g_1$ ,  $g_2$  and  $g_3$  polarized directions, respectively. The real part of refractive index  $n(\omega)$  had a minimal value at 2.98 eV, 3.05 eV and 3.09 eV along  $g_1$ ,  $g_2$  and  $g_3$  directions for  $\beta$ -PTCDA at a lower energy location, respectively; the imaginary part of refractive index  $k(\omega)$  had a maximal value at 2.40 eV, 2.49 eV and 2.50 eV along  $g_1$ ,  $g_2$  and  $g_3$  directions for  $\beta$ -PTCDA at a lower energy location, respectively. The minimal values of the real part  $n(\omega)$  and the maximal values of the imaginary part  $k(\omega)$  of the refractive index along  $g_1$  direction differed from those along  $g_2$  and  $g_3$  directions, which clearly showed the obvious anisotropy of  $\beta$ -PTCDA molecular crystal; this would lay a solid foundation for further study on its physical and chemical properties. Considering the refractive index of polycrystalline  $\beta$ -PTCDA, which was

equivalent to the average of the anisotropic refractive index here<sup>[36]</sup>, this also agreed with the experiment results in literature<sup>[37]</sup>.

The energy loss function is associated with the plasma oscillation, and the peak position corresponds to the plasma oscillation frequency<sup>[33]</sup>. For example, as shown in Fig. 8, the significant plasma oscillation frequency in  $g_1$  polarization direction is 17.23 eV, and is 18.15 and 18.33 eV in  $g_2$  and  $g_3$  polarization directions. Thus it can be seen that the resonance frequencies of the plasma oscillation in  $g_2$  and  $g_3$  polarization directions is different from that in  $g_1$  direction, which shows that the  $\beta$ -PTCDA molecular crystal has anisotropic conductivity.

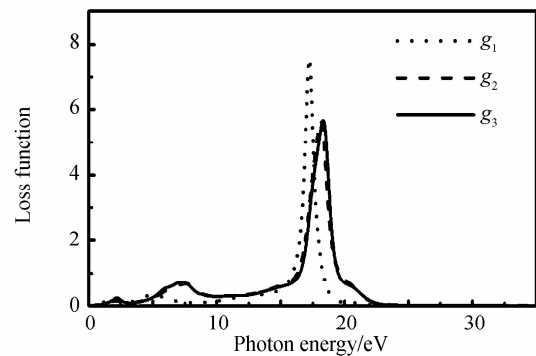


Fig. 8 Energy loss function of  $\beta$ -PTCDA molecular crystal

### 3 Conclusion

The first-principles calculations were performed based on the DFT to investigate the electronic structures and optical properties of  $\beta$ -PTCDA molecular crystal. The electronic band structure, PDOS, dielectric function, absorption coefficient, refractive

index and energy loss function were systematically investigated, its characteristics were interpreted, and the relations between them were discussed. As a consequence, these results were helpful in identifying the nature of the occupied and unoccupied states near  $E_F$  level, as well as the role of different kinds of atoms in shaping the optoelectronic properties. It can be seen that  $\pi$  electrons from perylene core together with O 2p states formed the top of valence band, and the C 2p and O 2p states formed the bottom of conduction band. These electronic states were close to the  $E_F$  and would provide most significant parameters in  $\beta$ -PTCDA organic semiconductor technology and application. Moreover, the obtained optical parameters provided comprehensive information about the  $\beta$ -PTCDA, such as the frequency dependence of anisotropic dielectric function, while the calculated real part  $\epsilon_1(\omega) < 0$  in a certain optical frequency range, which indicated that the conductivity was bigger in this optical frequency range, also was a reflection of the surface plasmon polariton, which was consistent with the energy loss function. From the anisotropic absorption and anisotropic refractive index, it could be concluded that  $\beta$ -PTCDA molecular crystal was optically biaxial. These results could provide an indispensable reference for further experimental studying in a wide frequency range.

#### Reference

- [1] DEDIU V A, HUESO L E, BERGENTI I, *et al.* Spin routes in organic semiconductors[J]. *Nature Material*, 2009, **8**(9): 707-716.
- [2] LUO Wei, ALLEN M, RAJU V, *et al.* An organic pigment as a high-performance cathode for sodium-ion batteries[J]. *Advanced Energy Materials*, 2014, **4**(15): 1-5.
- [3] HONG Jhen-yong, OU-YANG Kui-hon, WANG Bo-yao, *et al.* Interfacial spectroscopic characterization of organic/ferromagnet hetero-junction of 3, 4, 9, 10-perylenetetracarboxylic dianhydride-based organic spin valves [J]. *Applied Physics Letters*, 2014, **104**(8): 083301.
- [4] RAND B P, BURK D P, FORREST S R. Offset energies at organic semiconductor heterojunctions and their influence on the open-circuit voltage of thin-film solar cells[J]. *Physical Review B*, 2007, **75**(11): 115327.
- [5] WU Wei-ping, LIU Yun-qi, ZHU Dao-ben.  $\pi$ -Conjugated molecules with fused rings for organic field-effect transistors: design, synthesis and applications [J]. *Chemical Society Reviews*, 2010, **39**(5): 1489-1502.
- [6] WUESTEN J, ZIEGLER C, ERTL T. Electron transport in pristine and alkali metal doped perylene-3, 4, 9, 10-tetracarboxylic dianhydride (PTCDA) thin films [J]. *Physical Review B*, 2006, **74**(12): 125205.
- [7] KUMAR B, KAUSHIK B K, NEGI Y S. Perspectives and challenges for organic thin film transistors: materials, devices, processes and applications[J]. *Journal of Materials Science: Materials in Electronics*, 2014, **25**(1): 1-30.
- [8] HAN Yu-yan, NING Wei, DU Hai-feng, *et al.* Preparation, optical and electrical properties of PTCDA nanostructures[J]. *Nanoscale*, 2015, **7**(40): 17116-17121.
- [9] BARIŞ B, ÖZDEMİR H G, TUĞLUOĞLU N, *et al.* Optical dispersion and dielectric properties of rubrene organic semiconductor thin film[J]. *Journal of Materials Science: Materials in Electronics*, 2014, **25**(8): 3586-3593.
- [10] CHEN B S, LI Y Z, GUAN X Y, *et al.* First-principles study of structural, elastic and electronic properties of ZrIr alloy[J]. *Computational Materials Science*, 2015, **105**: 66-70.
- [11] BANNANI A, BOBISCH C, MÖLLER R. Ballistic electron microscopy of individual molecules[J]. *Science*, 2007, **315**(5820): 1824-1828.
- [12] BRUMME T, NEUCHEVA O A, TOHER C, *et al.* Dynamical bistability of single-molecule junctions: A combined experimental and theoretical study of PTCDA on Ag (111)[J]. *Physical Review B*, 2011, **84**(11): 115449.
- [13] ALONSO M I, GARRIGA M, KARL N, *et al.* Anisotropic optical properties of single crystalline PTCDA studied by spectroscopic ellipsometry[J]. *Organic Electronics*, 2002, **3**(1): 23-31.
- [14] SHARIFZADEH S, BILLER A, KRONIK L, *et al.* Quasiparticle and optical spectroscopy of the organic semiconductors pentacene and PTCDA from first principles [J]. *Physical Review B*, 2012, **85**(12): 125307.
- [15] OGAWA T, KUWAMOTO K, ISODA S, *et al.* 3, 4, 9, 10-Perylenetetracarboxylic dianhydride (PTCDA) by electron crystallography [J]. *Acta Crystallographica Section B: Structural Science*, 1999, **55**(1): 123-130.
- [16] SCHNEIDER M, UMBACH E, SOKOLOWSKI M. Growth-dependent optical properties of 3, 4, 9, 10-perylenetetracarboxylic acid-dianhydride (PTCDA) films on Ag (111)[J]. *Chemical Physics*, 2006, **325**(1): 185-192.
- [17] FERGUSON A J, JONES T S. Photophysics of PTCDA and Me-PTCDA thin films: Effects of growth temperature [J]. *The Journal of Physical Chemistry B*, 2006, **110**(13): 6891-6898.
- [18] HU Wen-cheng, LIU Yong , LI De-jiang, *et al.* Structural, anisotropic elastic and electronic properties of Sr - Zn binary system intermetallic compounds: A first-principles study[J]. *Computational Materials Science*, 2015, **99**: 381-389.
- [19] YANG Zhi-huai, ZHANG Yun-peng, KANG Cui-ping, *et al.* The first-principles study of electronic and optical properties of Co-Cr Co-doped rutile TiO<sub>2</sub>[J]. *Acta Photonica Sinica*, 2014, **43**(1): 0816002.
- [20] PERDEW J P, BURKE K, ERNZERHOF M. Generalized gradient approximation made simple[J]. *Physical Review Letters*, 1996, **77**(18): 3865-3867
- [21] ZHOU Jian, WANG Qian, SUN Qiang, *et al.* Electronic and magnetic properties of a BN sheet decorated with hydrogen and fluorine[J]. *Physical Review B*, 2010, **81**(8): 085442.
- [22] YANG Li-ming, RAVINDRAN P, VAJEESTON P, *et al.* A quantum mechanically guided view of Cd-MOF-5 from formation energy, chemical bonding, electronic structure, and optical properties [J]. *Microporous and Mesoporous Materials*, 2013, **175**: 50-58.
- [23] ZHAO Zong-yan , LI Zhao-sheng, ZOU Zhi-gang. Electronic structure and optical properties of monoclinic clinobisvanite BiVO<sub>4</sub>[J]. *Physical Chemistry Chemical Physics*, 2011, **13**(10): 4746-4753.
- [24] CHEN Dong, CHEN Zhe, WU Yi, *et al.* First-principles investigation of mechanical, electronic and optical properties of Al<sub>3</sub>Sc intermetallic compound under pressure [J].

- Computational Materials Science*, 2014, **91**: 165-172.
- [25] GANGILENKA V R, TITOVA L V, SMITH L M, *et al.* Selective excitation of exciton transitions in PTCDA crystals and films[J]. *Physical Review B*, 2010, **81**(15): 155208.
- [26] ZHAI Jin-hui, WAN A-jun, YU Dong-li, *et al.* Structural, electronic, and optical properties of ordered  $\text{Si}_{1-x}\text{Ge}_x\text{C}$  alloys: A first principles study[J]. *Journal of Alloys and Compounds*, 2015, **632**: 629-633.
- [27] WANG Qing-bo, ZHOU Cui, CHEN Ling, *et al.* The optical properties of NiAs phase ZnO under pressure calculated by GGA+U method[J]. *Optics Communications*, 2014, **312**: 185-191.
- [28] WENG Hong-ming, YANG Xiao-ping, DONG Jin-ming, *et al.* Electronic structure and optical properties of the Co-doped anatase  $\text{TiO}_2$  studied from first principles[J]. *Physical Review B*, 2004, **69**(12): 125219.
- [29] LEI Chen, YANG Zhi-hua, ZHANG Bing-bing, *et al.* The influence of hydrogen bonding on the nonlinear optical properties of a semiorganic material  $\text{NH}_4\text{B}[\text{d}(+)\text{-C}_4\text{H}_4\text{O}_5]_2 \cdot \text{H}_2\text{O}$ : a theoretical perspective[J]. *Physical Chemistry Chemical Physics*, 2014, **16**(37): 20089-20096.
- [30] HUANG Yu-hong, ZHANG Zong-quan, MA Fei, *et al.* First-principles calculation of the band structure, electronic states, and optical properties of Cr-doped ZnS double-wall nanotubes[J]. *Computational Materials Science*, 2015, **101**: 1-7.
- [31] KHAN M, XU Jun-na, CHEN Ning, *et al.* First principle calculations of the electronic and optical properties of pure and (Mo, N) co-doped anatase  $\text{TiO}_2$ [J]. *Journal of Alloys and Compounds*, 2012, **513**: 539-545.
- [32] LI Yan-lu, ZHAO Xian, FAN Wei-liu. Structural, electronic, and optical properties of Ag-doped ZnO nanowires; first principles study [J]. *The Journal of Physical Chemistry C*, 2011, **115**(9): 3552-3557.
- [33] CEN Wei-fu, YANG Yin-ye, FAN Meng-hui, *et al.* Electronic structure and optical properties of orthorhombic P-doped  $\text{Ca}_2\text{Si}$  calculated by the first-principles [J]. *Acta Photonica Sinica*, 2014, **43**(8): 0816002.
- [34] BULOVIC V, BURROWS P E, FORREST S R, *et al.* Study of localized and extended excitons in 3, 4, 9, 10-perylenetetracarboxylic dianhydride (PTCDA) I. Spectroscopic properties of thin films and solutions [J]. *Chemical Physics*, 1996, **210**(1): 1-12.
- [35] GUO G Y, CHU K C, WANG Ding-sheng, *et al.* Linear and nonlinear optical properties of carbon nanotubes from first-principles calculations[J]. *Physical Review B*, 2004, **69**(20): 205416.
- [36] VRAGOVIC I, SCHOLZ R. Frenkel exciton model of optical absorption and photoluminescence in  $\alpha$ -PTCDA[J]. *Physical Review B*, 2003, **68**(15): 155202.
- [37] CISOWSKI J, JARZABEK B, JURUSIK J, *et al.* Direct determination of the refraction index normal dispersion for thin films of 3, 4, 9, 10-perylene tetracarboxylic dianhydride (PTCDA)[J]. *Optica Applicata*, 2012, **42**(1): 181-192.